ATP-sensitive K^+ channels: regulation of bursting by the sulphonylurea receptor, PIP_2 and regions of Kir6.2

Bernard Ribalet[1,2], Scott A. John[1,3], Lai-Hua Xie[1,3] and James N. Weiss[1,2,3]

[1] *University of California Los Angeles Cardiovascular Research Laboratory and* [2] *Departments of Physiology and* [3] *Medicine (Cardiology), David Geffen School of Medicine at University of California Los Angeles, Los Angeles, CA 90095, USA*

ATP-sensitive K^+ channels composed of the pore-forming protein Kir6.2 and the sulphonylurea receptor SUR1 are inhibited by ATP and activated by Phosphatidylinositol Bisphosphate (PIP_2). Residues involved in binding of these ligands to the Kir6.2 cytoplasmic domain have been identified, and it has been hypothesized that gating mechanisms involve conformational changes in the regions of the bundle crossing and/or the selectivity filter of Kir6.2. Regulation of Kir6.2 by SUR1, however, is not well-understood, even though this process is ATP and PIP_2 dependent. In this study, we investigated the relationship between channel regulation by SUR1 and PIP_2 by comparing a number of single and double mutants known to affect open probability (P_o), PIP_2 affinity, and sulphonylurea and MgADP sensitivity. When coexpressed with SUR1, the Kir6.2 mutant C166A, which is characterized by a P_o value close to 0.8, exhibits no sulphonylurea or MgADP sensitivity. However, when P_o was reduced by combining mutations at the PIP_2-sensitive residues R176 and R177 with C166A, sulphonylurea and MgADP sensitivities were restored. These effects correlated with a dramatic decrease in PIP_2 affinity, as assessed by PIP_2-induced channel reactivation and inhibition by neomycin, an antagonist of PIP_2 binding. Based on macroscopic and single-channel data, we propose a model in which entry into the high-P_o bursting state by the C166A mutation or by SUR1 depends on the interaction of PIP_2 with R176 and R177 and, to a lesser extent, R54. In conjunction with this PIP_2-dependent process, SUR1 also regulates channel activity via a PIP_2-independent, but MgADP-dependent process.

(Resubmitted 25 October 2005; accepted after revision 16 December 2005; first published online 22 December 2005)
Corresponding author B. Ribalet: Department of Physiology, School of Medicine, University of California Los Angeles, Los Angeles, CA 90095, USA. Email: bribalet@mednet.ucla.edu

ATP-sensitive K^+ (K_{ATP}) channels are inhibited by ATP and activated by PIP_2. These two opposing processes are interrelated, because PIP_2 decreases ATP sensitivity (Baukrowitz *et al.* 1998; Fan & Makielski, 1999; Koster *et al.* 1999*b*; Ribalet *et al.* 2000). It has been suggested that competition between ATP and PIP_2 for binding to K_{ATP} channels may account for the decrease in ATP sensitivity evoked by PIP_2 (Shyng *et al.* 2000; MacGregor *et al.* 2002); however, other data suggest that the two ligand binding sites have no common residues (Ribalet *et al.* 2003; Schulze *et al.* 2003). Therefore, the decrease in ATP sensitivity evoked by PIP_2 may not be due to a direct competition of the two ligands for one site. PIP_2 also affects the interaction of the sulphonylurea receptor SUR1 with the pore-forming protein Kir6.2, causing functional uncoupling between the two subunits, as manifested by loss of channel inhibition by the sulphonylurea glibenclamide and reactivation by MgADP (Koster *et al.* 1999*b*; Ribalet *et al.* 2000). Whether this effect is due to direct interaction of PIP_2 with SUR1 regulatory sites, or mediated through another effect, such as the increase in open probability (P_o) evoked by PIP_2, is still unclear. Our work presented here addresses this issue.

Based on data from mutagenesis experiments and the published structure of inward rectifier K^+ channels (Nishida & MacKinnon, 2002; Kuo *et al.* 2003), the residues that interact with PIP_2 are part of the pore-forming protein Kir6.2 and may be divided into two groups. One group is located near the membrane, potentially interacting with PIP_2 directly. These residues are highly conserved throughout the Kir channel family, and include (at equivalent sites relative to Kir6.2) R54 in the N-terminus (Schulze *et al.* 2003), and R176, R177 and R206 in the C-terminus (Fan & Makielski, 1997; Shyng *et al.* 2000; John *et al.* 2001). The second more diversified group includes residues which appear too far away from the membrane to interact with PIP_2 directly, but may alter protein conformation and allosterically affect the interaction of PIP_2 with the former group of residues. This group includes R314 and E229 (Lin *et al.* 2003), which form inter-

 DOI: 10.1113/jphysiol.2005.100719

subunit interactions between C-tails of the Kir tetramer. Based on these findings, Lin *et al.* (2003) proposed a model whereby intersubunit interactions stabilize the tetramer, which in turn facilitates channel interaction with PIP_2, in order to achieve a high P_o.

Among the first group of directly interacting PIP_2-sensitive residues, it has been previously proposed that R176 and R177 play a crucial role in the functional coupling of Kir6.2 to SUR. Thus, Kir6.2 R176C and R177C mutations prevent channel reactivation by MgADP and inhibition by sulphonylureas, suggesting uncoupling of Kir6.2 and SUR1 (John *et al.* 2001). However, experiments carried out with another R176 mutant, R176A, yielded opposite results with the channel exhibiting greater sensitivity to sulphonylureas (Koster *et al.* 1999*b*). To further address this issue, we examined in the present study mutants of R176 and R177, as well as R54, to investigate how PIP_2 affects the coupling between Kir6.2 and SUR1. R206 mutations did not generate measurable currents, even though normally inserted into the plasma membrane, and so could not be characterized. To assess PIP_2 sensitivity of the various mutant channels, we investigated the degree of channel reactivation by exogenous PIP_2 and corroborated these results with data obtained with the PIP_2 antagonist neomycin, which inhibits the interaction of PIP_2 with positively charged residues (Fan & Makielski, 1997; Schulze *et al.* 2003). A close inverse relationship exists between the data obtained with exogenous PIP_2 and those obtained in the presence of its antagonist, neomycin, suggesting that low sensitivity to neomycin reflects high PIP_2 affinity, and high sensitivity reflects low PIP_2 affinity.

Based on our findings, we present evidence for a model where C166A facilitates entry into the high-P_o bursting state ($P_o > 0.8$), in a manner similar to SUR1 by favouring the interaction of PIP_2 with R176, R177 and, to a lesser extent, R54. Based on the proximity of R176 and R177 to the bundle crossing region, our data are consistent with the previously proposed hypothesis that PIP_2 binding stabilizes the bundle crossing in a conformation corresponding to the bursting state of the channel (Fan & Makielski, 1999; Enkvetchakul *et al.* 2000).

Methods

The techniques for cDNA expression and patch-clamp recording have been previously described in detail (John *et al.* 1998) and are only briefly outlined here.

Molecular biology and cDNA expression in HEK293 cells

HEK293 cells were transfected with cDNA for Kir6.2 mutants linked to Green Flourescent Protein (GFP) at the C-terminus (Kir6.2–GFP) so that insertion of the constructs into the plasma membrane could be investigated. Our previous findings showed that linkage to GFP did not affect the kinetics or adenine nucleotide sensitivity of wild-type Kir6.2 + SUR1 channels (John *et al.* 1998). All wild-type cDNAs were subcloned into the vector pCDNA3amp (Invitrogen). cDNAs used to make the GFP chimeras were subcloned into the plasmid Enhanced Green Flourecent Protein (pEGFP) vector. Both vectors used the cytomegalovirus (CMV) promoter. Single-site Kir6.2 mutations were constructed using the 'Quickchange' technique from Stratagene (La Jolla, CA, USA). The transfections were carried out using the calcium phosphate precipitation method (Graham & van der Eb, 1973). Expression of proteins linked to GFP was detected as early as 12 h after transfection. Patch-clamp experiments were started approximately 30 h after transfection. HEK293 cells were cultured in high-glucose Dulbecco's modified Eagle's medium (DMEM) supplemented with 10% (v/v) fetal calf serum, penicillin (100 units ml^{-1}), streptomycin (100 units ml^{-1}) and 2 mM glutamine, and divided once a week by treatment with trypsin.

Patch-clamp methods

Currents were recorded in HEK293 cells using the inside-out patch-clamp configuration, with the pipette solution containing (mM): KCl 140, NaCl 10, $MgCl_2$ 1.1 and Hepes 10; pH adjusted to 7.2 with KOH. The bath solution consisted of (mM): KCl 140, NaCl 10, $MgCl_2$ 1.1, Hepes 10 and EGTA 5; pH adjusted to 7.2 with KOH. Patch pipettes pulled with Garner glass (Indian Hill, Claremont, CA, USA) type 7052 had a resistance of about 5 MΩ. Recordings of macroscopic currents were carried out at holding membrane potentials of −20 to −40 mV.

Current recordings and data analysis

The data, filtered at 2 kHz with an 8-pole Bessel filter, were recorded with a List EPC 7 (Darmstadt, Germany) patch-clamp amplifier and recorded on videotape at a fixed frequency of 44 kHz after digitization with a digital audio processor. For single-channel data analysis, the data were sampled at a rate of 5.5 kHz and analysed using pCLAMP 9.2 software (Axon Instruments Inc.). Analysis of burst duration was carried out using the acceptance/rejection interval method. Data are presented as mean ± S.E.M. In Table 1 the percentage values are generated using areas fitted under each component. The long open-time constant and short closed-time constant were best determined using data obtained with the C166A mutant. The short open-time constant was determined using data obtained with wild-type Kir6.2 channels in the

Table 1. Kinetics of wild-type and mutant Kir6.2 channels with and without SUR1

	Open time			Closed time			Burst duration (ms)	Openings per burst
	Short open time τ_{o1} (ms)	Long open time τ_{o2} (ms)	percent o2	Short closed time τ_{c1} (ms)	Long closed time τ_{c2} (ms)	percent c2		
Kir6.2 C166A without SUR1	0.71 ± 0.02	2.2 ± 0.15	~100%	0.6 ± 0.1	15 ± 4	2.5 ± 1.5%	432 ± 138	190 ± 90
		2.5 ± 0.12	*99 ± 0.5%*	*0.61 ± 0.04*	*15.5 ± 0.04*	*2 ± 0.5%*	*354 ± 55*	
Kir6.2C166A/ R176E/R177E + SUR1	0.74 ± 0.2	2.5 ± 0.5	21 ± 9%	0.8 ± 0.2	18 ± 5 17 ± 0.3	73 ± 13%	11 ± 4	4.2 ± 1
	0.77 ± 0.02	*2.2 ± 0.09*	*27 ± 0.6%*	*0.62 ± 0.08*		*76 ± 1.2%*	*5.5 ± 1.6*	
Kir6.2R54E + SUR1	0.82 ± 0.2	2.35 ± 0.2	42 ± 11%	0.67 ± 0.9	23 ± 7.2	6.5 ± 2%	31 ± 15 44 ± 5	12 ± 2.4
	0.67 ± 0.01	*2.3 ± 0.14*	*78 ± 1%*	*0.61 ± 0.01*	*22 ± 0.03*	*26 ± 1.4%*		
Kir6.2 without SUR1	0.7 ± 0.15	2.1 ± 0.1	28 ± 7%	0.7 ± 0.2	13 ± 4	76 ± 15%	5.6 ± 1.2	2.2 ± 0.8
	0.8 ± 0.02	*2 ± 0.2*	*14 ± 0.04%*	*0.61 ± 0.01*	*11.5 ± 0.1*	*91 ± 0.02%*	*6.2 ± 0.7*	
Kir6.2 + SUR1	0.65 ± 0.1	2.6 ± 0.3	84 ± 12%	0.6 ± 0.1	14 ± 3 14.5 ± 0.5	21 ± 14%	51 ± 25 55 ± 6	20 ± 6
	0.75 ± 0.03	*2.35 ± 0.03*	*94 ± 2%*	*0.61 ± 0.42*		*11 ± 3%*		

In each cell the numbers in italic are fitted values using the kinetic model in Fig. 10. The other numbers are experimental values, reflecting at least 3 experiments for each case.

absence of SUR1 or with C166A/R176E/R177E + SUR1 where channels exhibited primarily fast gating behaviour. These values were then used for model optimization as described below. For R54X + SUR1, which exhibit a mixture of the two types of opening, a two-exponential fit was often obtained.

Simulation of single-channel data with kinetic models

Simulation and fitting of single-channel data was carried out with the QuB suite of programs (University at Buffalo, the State University of New York, NY, USA) following the instructions provided with the program tutorials. Briefly, pCLAMP data files (.ldt) were first idealized using either the half amplitude or the segmental k-means (SKM) method (QuB software also allows transfer of records previously idealized using pCLAMP). After generation of the model to be tested and setting of the initial values for the rate constants, model optimization for kinetic analysis was carried out using the maximum interval likelihood (MIL) function. This function permits some control of parameter variation and generates an estimate of the variable rate constants (see Fig. 9). Single-channel data events could then be generated based on the estimated values, using the simulation (SIM) function and compared with the experimental data (see Fig. 9) to establish the validity of the kinetic model.

To measure ATP sensitivity, adenine nucleotides were added directly to the bath. First, ATP sensitivity was assessed prior to channel run-down as membrane patches were excised in the presence of 5 mM EGTA and 200 μM MgADP. To estimate the effect of run-down on ATP sensitivity, patches were exposed to Mg^{2+}-free solutions or to 200 nM glybenclamide to decrease P_o. As previously reported (Ribalet *et al.* 2003), these methods provide similar estimates of ATP sensitivity before and after spontaneous channel run-down, with the advantage of allowing rapid assessment of the effects of P_o on channel ATP sensitivity. PIP_2 (Calbiochem) was sonicated before use.

Results

Effect of P_o and PIP_2 on sulphonylurea and MgADP sensitivity

In the absence of SUR1, wild-type Kir6.2 channels exhibit brief openings with a low P_o near 0.1; when coexpressed with SUR1, the channel opens in longer bursts and P_o increases to 0.4–0.5 (Tucker *et al.* 1997; John *et al.* 1998). Furthermore, in the presence of SUR1, MgADP increases P_o further (Alekseev *et al.* 1998) and sulphonylureas prevent this stimulatory effect of MgADP, blocking channel activity partially by 37 ± 6%. This phenomenon is referred to as functional uncoupling (Koster *et al.* 1999*b*; Ribalet *et al.* 2000). Trapp *et al.* (1998) first reported that the Kir6.2 mutant channels, C166S or C166A, exhibited constant bursts of openings with P_o near 0.8 in the absence of SUR. Figure 1 shows that, when coexpressed with SUR1, these mutant channels show little or no sensitivity to the sulphonylurea glibenclamide or to reactivation by MgADP. In these experiments, inside-out membrane patches from HEK293 cells coexpressing Kir6.2166A + SUR1 channels were excised into a bath solution containing EGTA and 200 μM MgADP. MgADP was then removed, and ATP sensitivity was tested, yielding a half-maximal inhibition (IC_{50}) of 7.5 mM. In the presence of 2 mM ATP, MgADP caused almost no channel reactivation (Fig. 1*A*), and 200 nM glibenclamide had almost no inhibitory effect (< 5%, Fig. 1*B*). However, after exposure to glibenclamide, ATP sensitivity increased dramatically, with the IC_{50} decreasing to 1 mM.

It is generally accepted that a decrease in channel P_o causes an increase in ATP sensitivity. However, because the relationship between P_o and the ATP blocking potency is highly non-linear when the channel is operating near its maximal P_o (0.8–0.9), as is the case for C166A channels

(Enkvetchakul *et al.* 2000), the increase in ATP sensitivity after exposure to glibenclamide in C166A channels might be related to a subtle glibenclamide-induced decrease in P_o, below our ability to detect, rather than to an effect of the sulphonylurea independent of P_o. To investigate this possibility, we attempted to reduce the P_o of C166A channels by combining the C166A mutation with the mutations R176E or R176E/R177E. The R176E and R177E single mutants yielded no currents when expressed with or without SUR1, but the double mutant C166A/R176E + SUR1 (Fig. 2*A*–*C*), and to a lesser extent the triple mutant C166A/R176E/R177E + SUR1 (Fig. 2*D*), yielded currents which were smaller than with C166A in the absence of SUR1, suggesting P_o values lower than the value of 0.8–0.9 in C166A. This is supported by our observation that the channel density estimated using plasma membrane labelling with wild-type and Kir6.2 mutants linked to GFP was similar with C166A + SUR1 and C166A/R176E/R177E + SUR1. Thus, the C166A mutation rescued R176E and R176E/R177E currents.

Because the number of active channels was large, we were not able to obtain single channel recordings to measure directly the P_o of the double mutant C166A/R176E + SUR1. However, with the triple mutation C166A/R176E/R177E + SUR1, channel activity was dramatically decreased and a P_o approaching 0.1 could be measured from single-channel recordings (Fig. 3*B*), supporting our hypothesis that the mutations R176E and/or R177E combined with C166A have profound effects on channel P_o.

The ATP sensitivity of C166A/R176E + SUR1 channels was also higher than that of C166A + SUR1 channels,

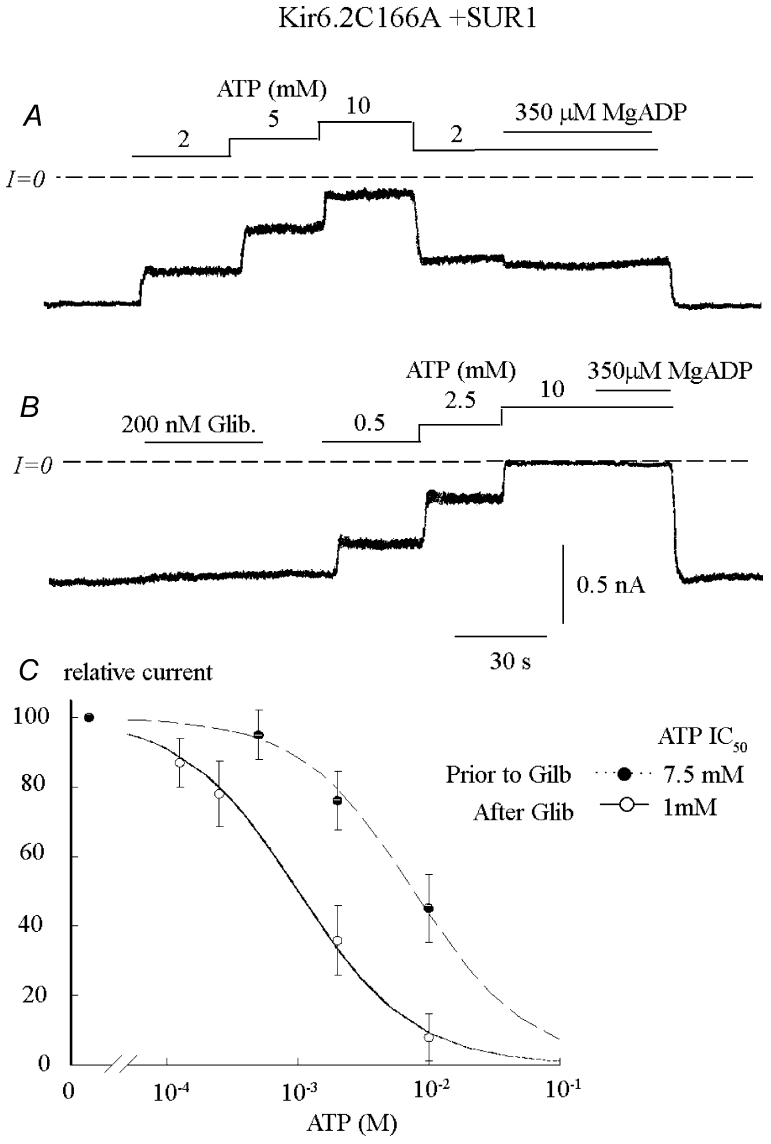

Figure 1. ATP and MgADP sensitivity of C166A mutant channels coexpressed with SUR1 before and after addition of glibenclamide
Current traces in the two upper panels depict inward currents measured before (*A*) and after (*B*) application of 200 nM glibenclamide. Currents were progressively suppressed by increasing ATP concentrations, with the half-maximal inhibition (IC_{50}) approximately 7.5 mM and 1 mM, respectively. The main observations are that C166A + SUR1 channels are poorly sensitive to MgADP (*A*) and the sulphonylurea glibenclamide (*B*). However, a small change in P_o due to glibenclamide (*B*) causes a dramatic increase in ATP sensitivity. *C*, graph showing ATP sensitivity for C166A + SUR1 channels before (●) and after (○) application of glibenclamide. Fit of the data points to the Hill equation yielded IC_{50} values of 7.5 mM ($n = 5$) before and 1 mM ($n = 4$) after addition of glibenclamide. In both cases the Hill coefficients were close to unity.

with an IC_{50} close to 1.5 mM prior to run-down (Fig. 2*A*). Furthermore, subsequent addition of MgADP reactivated channel activity by $18 \pm 4\%$ ($n = 4$) and decreased ATP sensitivity, unlike in C166A + SUR1 channels. Also unlike in C166A + SUR1 channels, glibenclamide had a potent inhibitory effect, blocking channel activity by $60 \pm 28\%$ ($n = 4$), and P_o remained depressed after washout of glibenclamide. After washout of glibenclamide, ATP sensitivity increased dramatically (IC_{50}, 57 μM), and MgADP no longer reactivated the channels (data not shown), consistent with glibenclamide causing functional uncoupling of Kir6.2 and SUR1.

For the triple mutant C166A/R176E/R177E coexpressed with SUR1, channel activity ran-down within 30 s after patch excision, but could also be activated by MgADP and inhibited by the sulphonylurea glibenclamide. In this case, channel inhibition by glibenclamide was almost complete and reached $89 \pm 4\%$ ($n = 4$) (Fig. 2*D*).

Thus, when the intrinsic P_o of the C166A channel was reduced by also mutating R176 and/or R177, the dependence of sulphonylureas and MgADP sensitivity on channel P_o became apparent. These results suggest that C166A does not directly disrupt functional coupling between Kir6.2 and SUR1: rather, the low sulphonylurea and MgADP sensitivities of C166A + SUR1 channels are related to the very high intrinsic P_o of this mutant. Further support for this idea was obtained with C166V + SUR1 channels, which have a P_o close to that of wild-type; in the absence of SUR1, both wild-type and C166V mutant channels have a P_o of 0.1 (Trapp *et al.* 1998). Channel

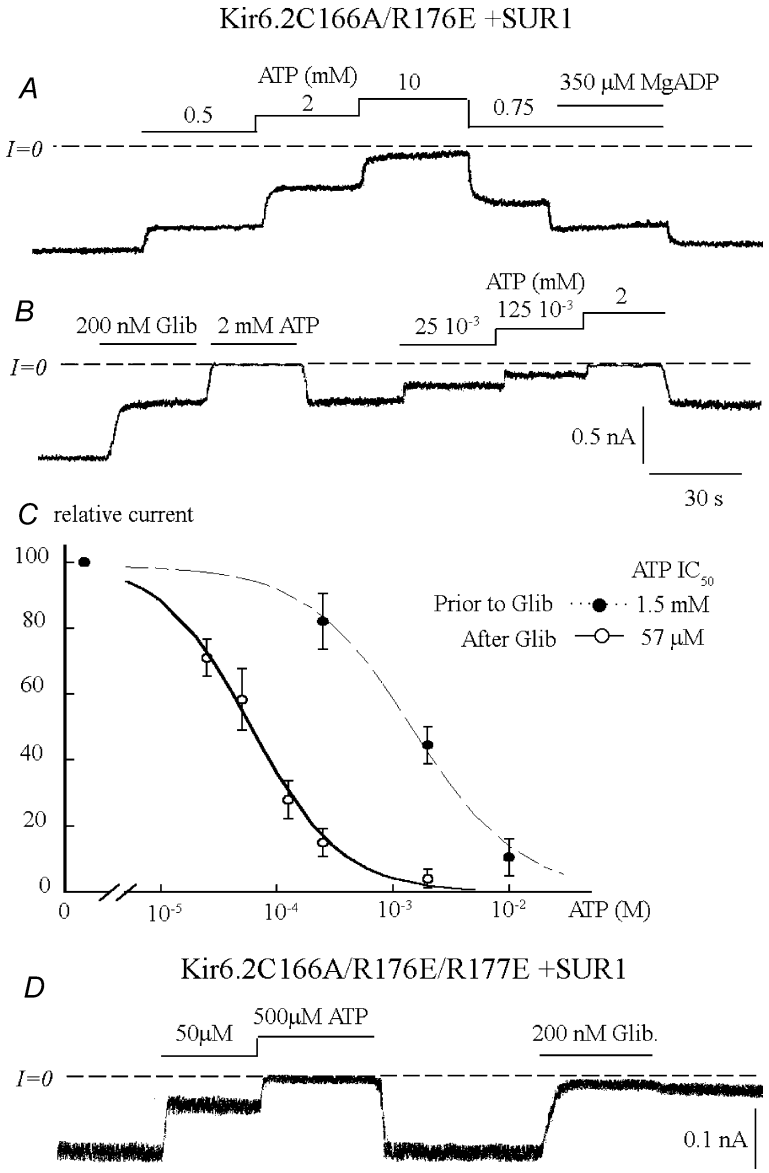

Figure 2. Properties of C166A/R176E (*A–C*) and C166A/R176E/R177E channels (*D*) coexpressed with SUR1 before and after addition of glibenclamide
Current traces in the two upper panels depict inward currents from C166A/R176E + SUR1 channels measured before (*A*) and after (*B*) application of 200 nM glibenclamide. Currents were progressively suppressed by increasing ATP concentrations, with IC_{50} values near 1.5 mM and 50 μM, respectively. In contrast to C166A + SUR1 channels (Fig. 1), C166A/R176E + SUR1 channels demonstrate high sensitivity to MgADP (*A*) and the sulphonylurea glibenclamide (*B*). Like C166A + SUR1 channels (Fig. 1), exposure to glibenclamide causes a dramatic increase in ATP sensitivity. *C*, graph showing ATP sensitivity for C166A/R176E + SUR1 channels before (●) and after (○) application of glibenclamide. Fit of the data points to the Hill equation yielded IC_{50} values of 1.5 mM ($n = 4$) before and 57 μM ($n = 3$) after application of glibenclamide. The two Hill coefficients were close to unity. *D*, inward current recording from C166A/R176E/R177E + SUR1 channels. The current amplitude was greatly diminished as compared to *A* and *B*, and inhibition by glibenclamide exceeded 90%. The channel sensitivity to ATP was similar to C166A-R176E + SUR1 channels after addition of glibenclamide, with an IC_{50} of 45 μM.

activity was reactivated by MgADP and inhibited by sulphonylureas by 45%, a value similar to that observed with wild-type channels. Other mutants such as C166L, which have intermediary P_o, also exhibited intermediate MgADP and sulphonylurea sensitivities (data not shown). As R176 and R177 are involved in the interaction of PIP_2 with the channel, these findings also indicate that MgADP-dependent functional coupling between Kir6.2 and SUR1 is independent of the interaction of PIP_2 with R176/R177.

Effects of C166 and PIP_2-sensitive residues R176/R177 on bursting behaviour

The single-channel recordings in Fig. 3 are also revealing, because C166A channels exhibited almost continuous bursting (Fig. 3*A*), with few closed times between bursts, as previously described (Trapp *et al.* 1998). During bursts, open and closed times in C166A channels were well-fitted with single exponentials, with time constants of opening (τ_o) and closing (τ_c) of 2.2 ms and 0.6 ms, respectively, similar to those published for the bursting mode of wild-type Kir6.2 + SUR1 (Table 1). Unlike C166A channels, however, wild-type Kir6.2 channels require SUR1 to exhibit bursting behaviour, indicating that wild-type residue C166 does not favour normally the transition into the long bursting mode, and that SUR1 somehow facilitates this transition. In contrast, single-channel activity obtained with C166A/R176E/R177E + SUR1 exhibited short openings reminiscent of the fast gating of Kir6.2 without SUR1 (Table 1). The open-time histogram was well-fitted by a single exponential (τ_o, 0.75 ms), but in some cases a second exponential (τ, ~2.5 ms) contributing less than 25% of the fitted area, was observed. The closed-time histogram was fitted with two exponentials ($\tau_{c1} =$ 0.8 ms and $\tau_{c2} = 18$ ms). Thus, the kinetic behaviour of C166A/R176E/R177E + SUR1 is very similar to that of Kir6.2 in the absence of SUR1, for which

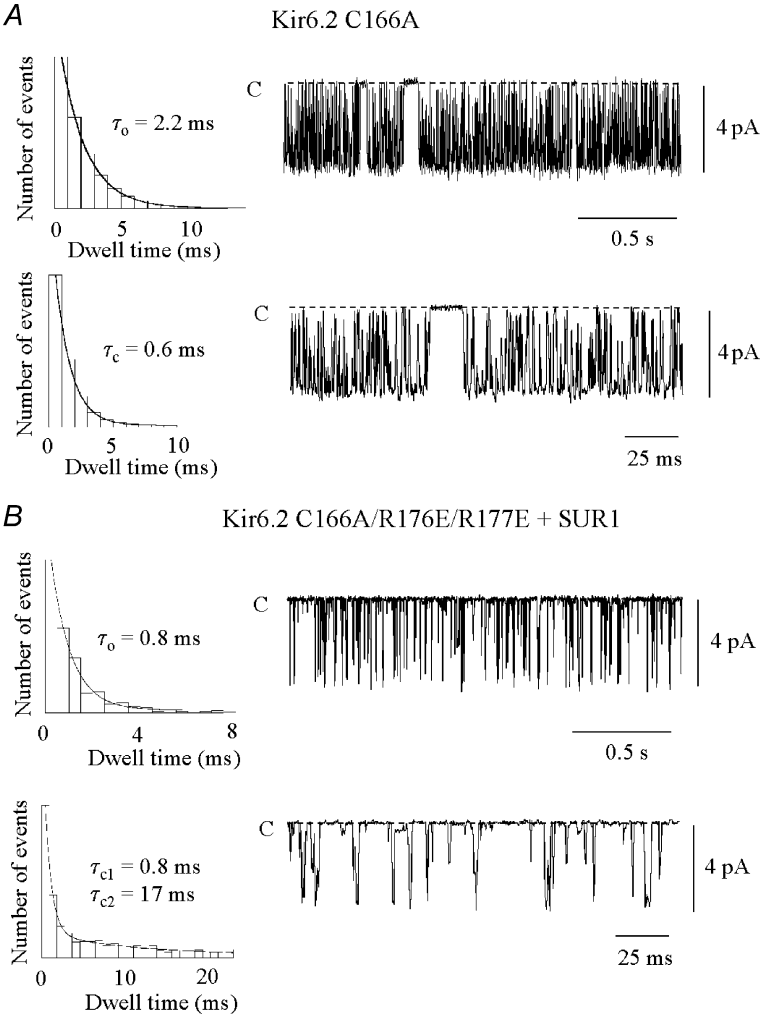

Figure 3. Single channel recordings from C166A and C166A/R176E/R177E channels
A, inward currents obtained with the C166A mutant were recorded in excised inside-out patches at a holding potential of −60 mV and are represented as downward deflections, showing bursts of openings. The lower trace shows single-channel recording on an expanded timescale. The open-time histogram on the top left was well-fitted with a single exponential ($\tau_o = 2.2$ ms). The closed-time histogram below required two exponentials ($\tau_{c1} = 0.6$ ms and $\tau_{c2} = 15$ ms). However, the slow (interburst) time constant component contributed little to the total number of events (see Table 1). In contrast, C166A/R176E/R177E channels opened only with short openings and demonstrated a fast gating behaviour (*B*) similar to wild-type Kir6.2 channels in the absence of SUR1. This behaviour is illustrated in the expanded lower single-channel current tracing. In this case the open-time histogram on the left was fitted by a single exponential ($\tau_o = 0.8$ ms), but a second slower time constant could also be observed (Table 1). The closed-time histogram below also required two exponentials ($\tau_{c1} = 0.8$ ms and $\tau_{c2} = 17$ ms).

the main open and closed time constants are near 0.7 ms and 13 ms, respectively (Table 1).

Based on these results, we conclude that interaction of PIP_2 with R176 and/or R177 is necessary for the generation of long bursts by both the C166A mutation and wild-type Kir6.2 channels coexpressed with SUR1, but not for functional coupling between Kir6.2 and SUR1.

It is interesting to note that, like R176E, R176A mutant channels exhibit MgADP and sulphonylurea sensitivity (data not shown), R176C mutants do not (John *et al.* 2001). On the basis of our previous data with R176C and R177C, we suggested that R176C and R177C prevented functional coupling between Kir6.2 and SUR1. The difference in functional coupling between R176A and R176E on one hand and R176C on the other hand may be accounted for by the difference in channel P_o recorded in the presence of SUR1. Indeed, we found that while the P_o of R176C mutant channels in the absence of SUR1 is similar to the low P_o of wild-type channels (John *et al.* 2001 and Fig. 4*A*), the P_o of R176C coexpressed with SUR1 is very high and approaches a maximum of 0.8 (Fig. 4*B*), a result which differs dramatically from the low P_o measured with R176E/R177E in the presence of SUR1. Further experiments will have to be carried out to establish the mechanism responsible for this difference between mutant R176C on the one hand and R176A, R176E on the other.

PIP_2 affinity in wild-type, C166A and C166A/R176E mutant channels

Our data obtained with C166A and C166A/R176E mutant channels indicate that the interaction of PIP_2 with R176/R177 is necessary for bursting. To further investigate this issue, we compared the ability of exogenous PIP_2 to reactivate these mutant channels after run-down. We also corroborated these data by investigating the effects of neomycin, which has been shown to antagonize the interaction with PIP_2 in a time- and concentration-dependent manner reflecting the affinity of the channels for PIP_2 (Fan & Makielski, 1997; Schulze *et al.* 2003). Inside-out patches from HEK293 cells coexpressing Kir6.2 + SUR1 were excised into a bath solution containing EGTA. Figure 5*A* and *D* illustrates channel reactivation by PIP_2 with C166A + SUR1 and C166A/R176E + SUR1 channels, respectively. Reactivation of C166A after Ca^{2+}-induced run-down was fast and robust, with half-time for

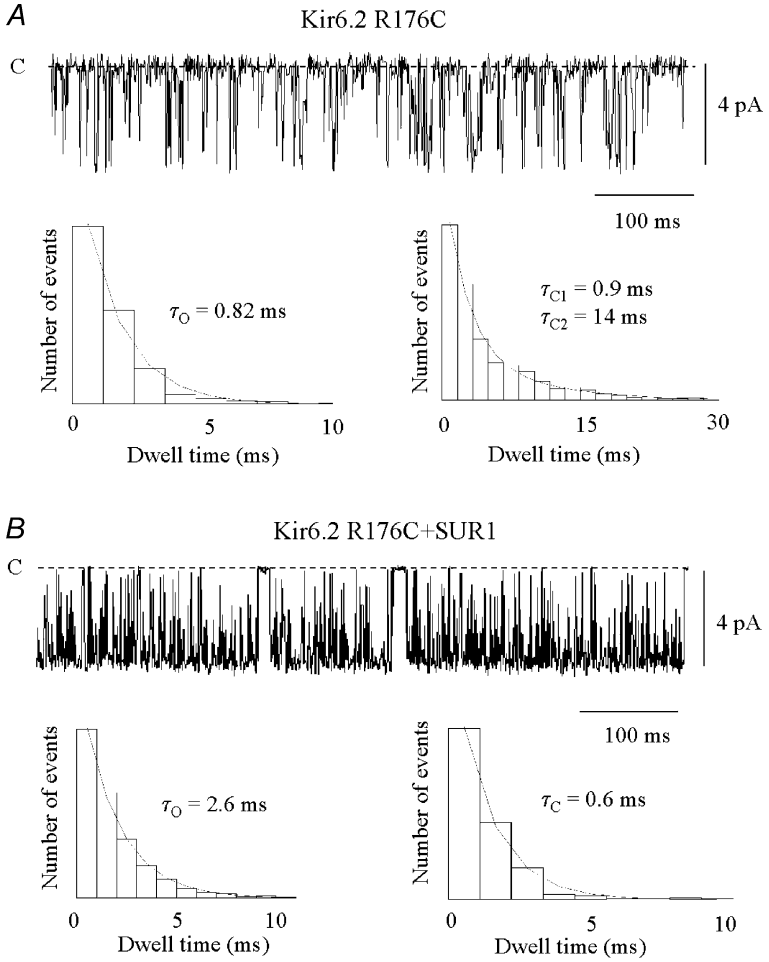

Figure 4. Single-channel recordings from R176C channels without and with SUR1
A, inward currents obtained with the R176C mutant were recorded in the absence of SUR1 in excised inside-out patches at a holding potential of −60 mV and are represented as downward deflections, showing brief openings. In this case the channel P_o was 0.13. The open-time histogram in the bottom left panel was fitted with a single exponential ($\tau_o = 0.82$ ms), while the closed-time histogram on the right required two exponentials ($\tau_{c1} = 0.9$ ms and $\tau_{c2} = 14$ ms). In contrast, in the presence of SUR1, R176C channels opened in a long burst (*B*). In this case channel P_o approached maximum (0.8). The open-time histogram in the bottom left panel was fitted by a single exponential ($\tau_o = 2.6$ ms) and the closed-time histogram on the right also required one exponential ($\tau_c = 0.6$ ms).

stimulation ($t_{1/2}$) averaging 21 ± 8 s. In contrast, the extent of C166A/R176E + SUR1 channel reactivation was much more variable and occurred more slowly with a $t_{1/2}$ of 70 ± 28 s. With C166A/R176E/R177E + SUR1 mutant channels, PIP_2 failed to reactivate channel activity in four out of eight patches; in two patches channel activity recovered to a level similar to that prior to run-down and in two others channel activity increased slowly ($t_{1/2}$, 180 s) to levels greater than control (Fig. 6).

To further investigate the sensitivity of the channels to PIP_2, we next examined the effects of neomycin on mutant channels. Figure 5*B* shows the effects of neomycin on the

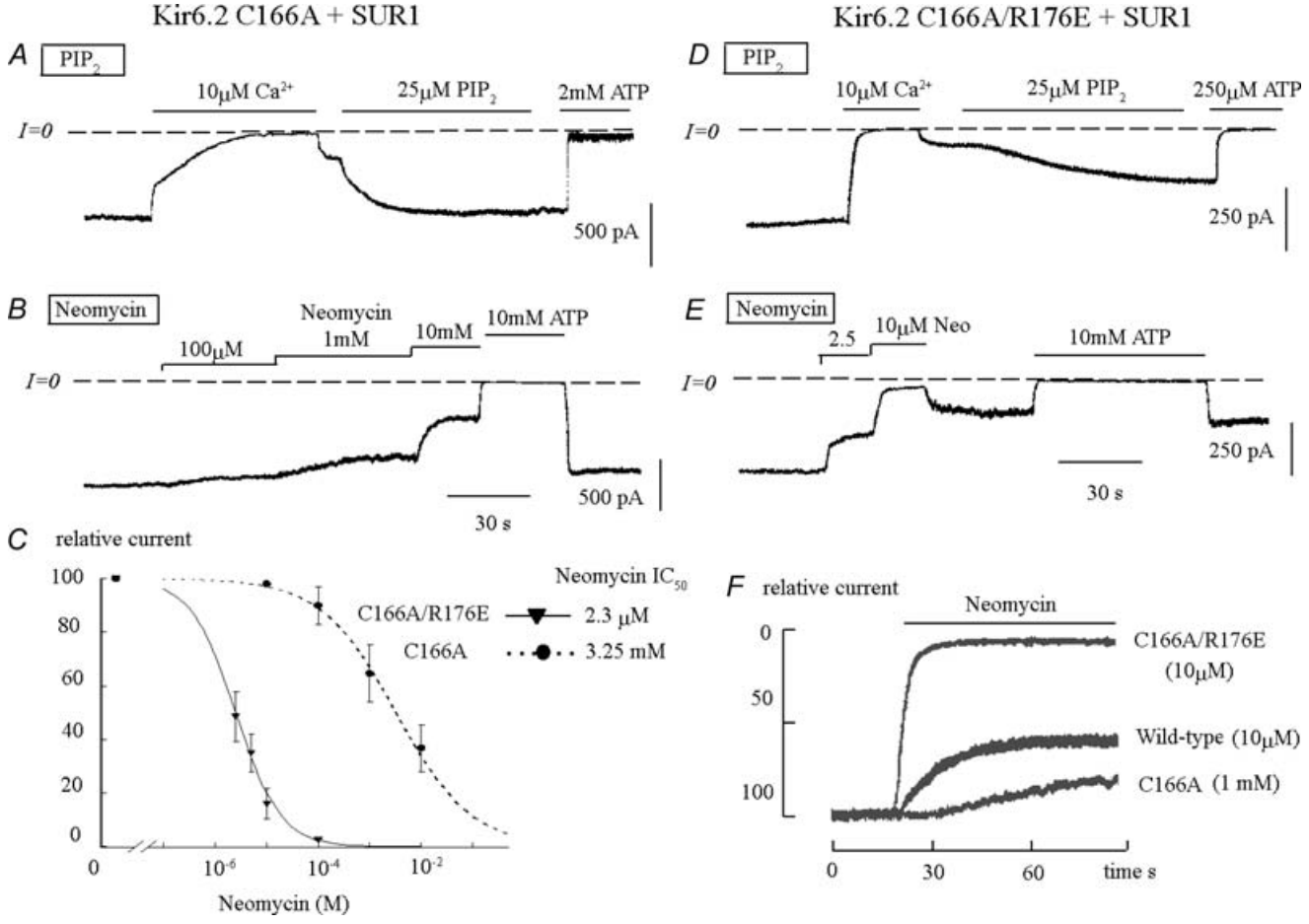

Figure 5. PIP_2 and neomycin sensitivity of Kir6.2 C166A + SUR1 and Kir6.2 C166A/R176E + SUR1 channels coexpressed with SUR1

Current traces in *A* and *D* illustrate the reactivation of Kir6.2 C166A and Kir6.2 C166A/R176E channels by PIP_2, respectively. *A*, the activity of C166A + SUR1 was first blocked by addition of Ca^{2+}. Upon removal of Ca^{2+}, there was partial recovery of channel activity; the level of recovery was dependent upon the duration of Ca^{2+} exposure. Addition of PIP_2 under these conditions caused full recovery of channel activity within 30 s. *D*, the activity of C166A/R176E + SUR1 was first blocked with Ca^{2+}; upon addition of PIP_2 there was only partial and slow recovery of channel activity consistent with low PIP_2 affinity. Also consistent with low PIP_2 affinity of C166A/R176E, we found that hydrolysis of PIP_2, as illustrated by Ca^{2+}-dependent rate of channel block, was much faster with the double mutant C166A/R176E + SUR1 as compared to with C166A + SUR1. data in *B* and *E* show how neomycin may be used to assess this difference in PIP_2 affinity and graphs in *C* and *F* illustrate how the effect of neomycin may be quantified. These data illustrate the potent increase in neomycin sensitivity elicited by R176E, which parallels the weak channel reactivation by PIP_2 in *D*. Consistent with the low PIP_2 affinity of C166A/R176E, 10 mM MgATP could restore only partially the activity of this channel (*E*), while reactivating fully C166A (*B*). *C*, fitting of the neomycin data points to the Hill equation yielded IC_{50} values of 3.25 mM ($n = 4$) for C166A + SUR1 (●) and 2.3 μM ($n = 4$) for C166A/R176E + SUR1 (▼). In both cases the Hill coefficients were less than unity. *F*, the rate of inhibition by neomycin is compared for C166A + SUR1 and C166A/R176E + SUR1 channels. In this example 10 μM neomycin caused 50% inhibition of C166A/R176E + SUR1 within 4 s, while 1 mM neomycin caused only gradual and partial inhibition of C166A + SUR1 over several minutes. The rate of inhibition of wild-type Kir6.2 channel by 10 μM neomycin is shown for comparison.

activity of C166A + SUR1 channels. With 10 and even 100 μM neomycin, there was almost no inhibitory effect, and substantial block occurred only at 1 mM and 10 mM. The IC_{50} for channel inhibition by neomycin was near 2.5 mM. This IC_{50} was much higher than that observed with wild-type channels (18 μM, data not shown), and upon removal of neomycin, there was almost complete recovery of channel activity with or without previous application of ATP. These results suggest a stronger interaction between the mutant channel and PIP_2 than in the wild-type channel. With C166A/R176E + SUR1 channels, the effect of neomycin was strikingly different (Fig. 5*E*) from the effect in C166A + SUR1 channels. Neomycin had a potent inhibitory effect (Fig. 5*C* and *E*) and half-maximal inhibition was increased about 1000-fold to 2.5 μM, which is less than with wild-type channels coexpressed with SUR1 (IC_{50}, 18 μM). In addition, the rate of inhibition increased dramatically (Fig. 5*F*) with 10 μM neomycin causing almost complete inhibition of C166A/R176E within less than 10 s, while 1 mM caused very gradual inhibition of C166A over several minutes, often without reaching saturation (Fig. 5*B* and *E*). Furthermore, there was little recovery of C166A/R176E + SUR1 channel activity after removal of neomycin and rejuvenation with MgATP was minimal, consistent with the low reactivation by PIP_2. These results are therefore consistent with R176 forming a strong interaction with PIP_2 in wild-type channels. Finally, the inverse relationship between reactivation by PIP_2 and inhibition by neomycin indicates that neomycin is a reliable tool to assess PIP_2 affinity.

To further investigate the role of the interaction of PIP_2 with R176/R177 in bursting, we studied the effect of run-down and PIP_2-induced reactivation on the kinetics of C166A/R176E/R177E mutant channels (Fig. 6). The upper panel illustrates the slow reactivation evoked by PIP_2 over several minutes. The expanded traces indicate that the increase in channel activity results from recruitment of previously inhibited channels following PIP_2 hydrolysis rather than increased mean channel open time. Alternatively, the increased activity may result from decreased closed time intervals (Fan & Makielski, 1999); however, in either case the lack of effect of PIP_2 on the open time supports our hypothesis whereby entry in the bursting mode requires interaction of PIP_2 with R176/R177.

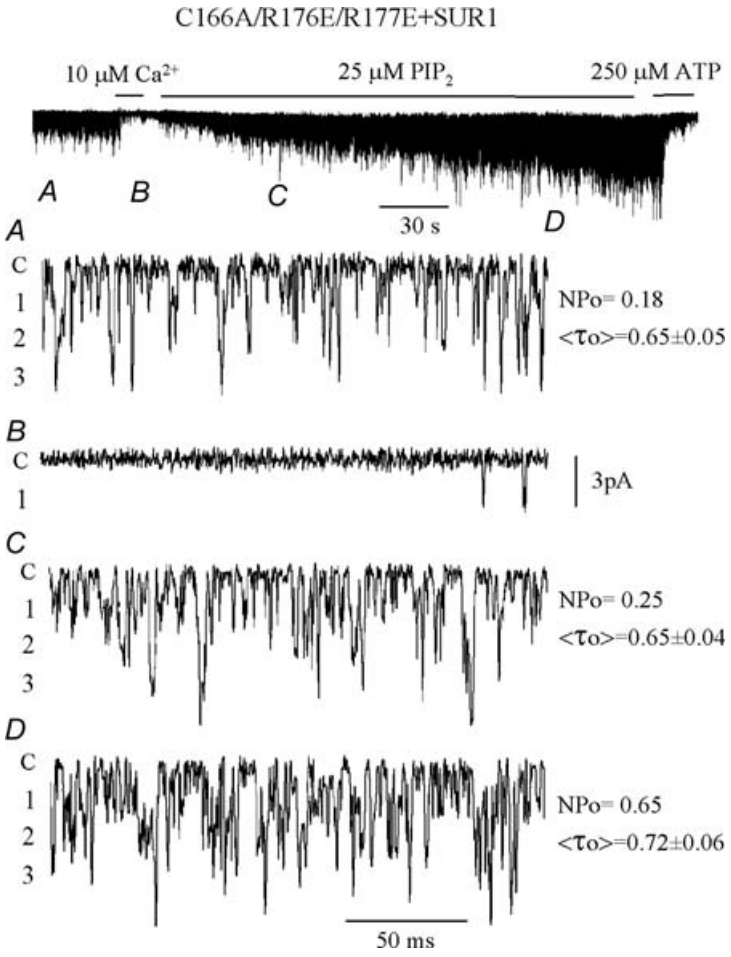

Figure 6. Effects on single channel kinetics of reactivation of C166A/R176E/R177E channels by PIP_2 in the absence of Mg^{2+}
Upper trace, inward currents obtained with the C166A/R176E/R177E mutant were recorded in excised inside-out patches at a holding potential of −60 mV and are represented as downward deflections. This recording illustrates the gradual increase in channel activity elicited by PIP_2 and the block by ATP. The lower four traces show single channel recording on an expanded timescale, before (*A*) and after application of PIP_2 (*C* and *D*). The values on the right of the traces illustrate the lack of effect of PIP_2 on the mean channel open time (compare *A* and *C*), thus, the increase in channel activity is probably due to channel recruitment. The mean open time was measured in all cases at the first level of opening and due to the presence of multiple channels in the patch the value of $<\tau_o>$ is not an accurate measurement of single-channel open time, but represents a compound value. The modest increment in $<\tau_o>$ in *D* reflects increased simultaneous opening of two or more channels.

All these data support the hypothesis that facilitation of channel entry into the long bursting mode by C166A is mediated via a strong interaction between R176/R177 and PIP_2. Similar results obtained with Kir6.2 coexpressed with SUR1 indicate that a comparable mechanism accounts for the bursts elicited by SUR1.

Regulation of PIP_2 binding and functional coupling by the N-terminus of Kir6.2

Thus far, our data indicate that the bursting behaviour evoked by C166A and SUR1 requires the interaction of the channel with PIP_2. However, we also found that in C166A/R176E + SUR1 channels, MgADP and the sulphonylurea glibenclamide had potent effects despite a very weakened PIP_2 interaction, suggesting that SUR1 may also regulate P_o via a PIP_2–independent process. To further investigate this hypothesis, we next studied mutations at R54 in the N-terminus of Kir6.2, which has been implicated as a PIP_2-sensitive residue (Schulze *et al.* 2003). It was previously reported (Schulze *et al.* 2003) that when R54Q and R54E were coexpressed with SUR1, channel activity was low and PIP_2 affinity was reduced, as indicated by a high sensitivity to neomycin (IC_{50}, ~3 μM). Figure 7*A* shows representative data obtained with the R54C + SUR1 channels. The IC_{50} for ATP was 320 μM (Fig. 7*A*), which is about 4-fold higher than the ATP sensitivity of wild-type channels prior to rundown (75 μM) (Ribalet *et al.* 2003), and the effect of glibenclamide was accentuated. MgADP reactivation was 44 ± 8% in seven patches and was similar to that of wild-type channels, while glibenclamide inhibition averaged 79 ± 13% compared to

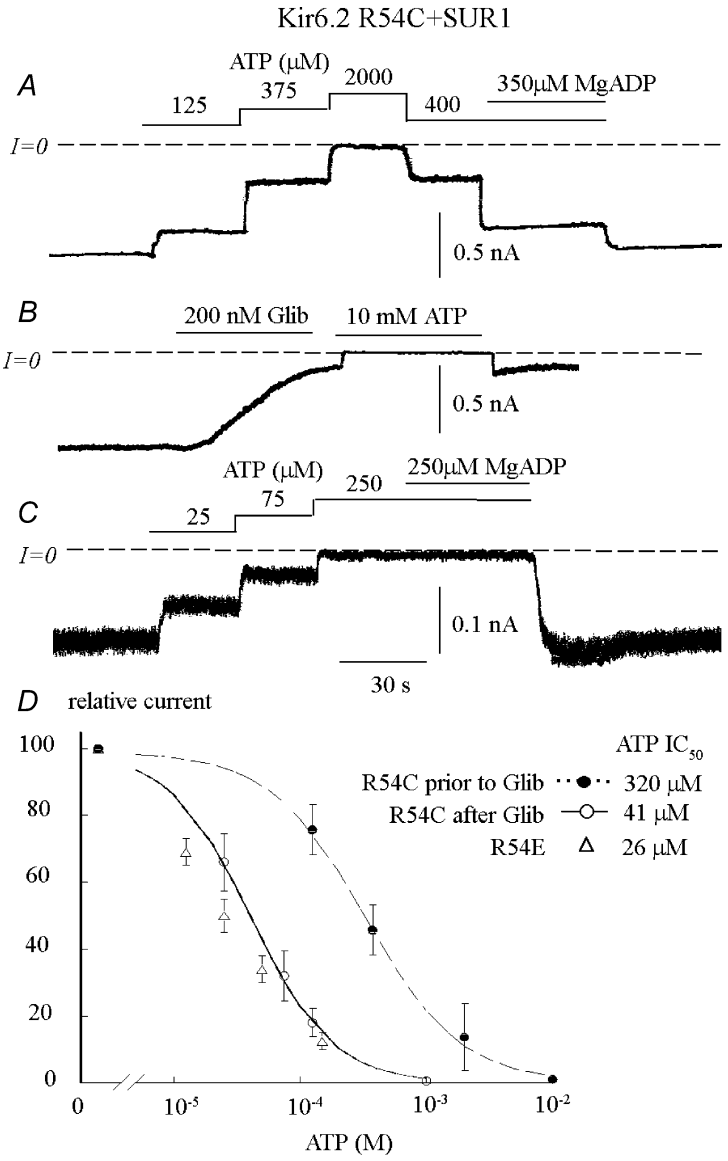

Figure 7. ATP and MgADP sensitivity of R54C and R54E channels coexpressed with SUR1, before and after addition of glibenclamide
Current traces depict inward currents measured before (*A*) and after (*B* and *C*) application of 200 nM glibenclamide. Currents were progressively suppressed by increasing ATP concentrations, with the IC_{50} values near 320 μM and 40 μM, respectively. R54C + SUR1 channels were reactivated by MgADP (*A*) and inhibited by the sulphonylurea glibenclamide (*B*). *D*, graph showing ATP sensitivity for R54C + SUR1 channels before (●) and after (○) application of glibenclamide. Fit of the data points to the Hill equation yielded IC_{50} values of 320 μM ($n = 5$) before and 41 μM ($n = 5$) after application of glibenclamide. In both cases the Hill coefficients were close to unity. *D* shows R54C + SUR1 data as well as data obtained with R54E + SUR1 channels. The IC_{50} for ATP of R54E + SUR1 channels was recorded after channel run-down. The small increase in ATP sensitivity from 41 to 26 μM with R54C and R54E, respectively, is likely to be due to the decreased P_o of R54E + SUR1 compared to R54C + SUR1 channels.

37% in wild-type channels (Fig. 7*B*). Also, as observed with wild-type channels, glibenclamide increased the ATP sensitivity by about 8-fold with the IC_{50} for ATP reaching 41 μM in this case (Fig. 7*C*). Similar results were obtained with R54A + SUR1 channels. In contrast, R54E + SUR1 channels ran-down rapidly (data not shown), and, although MgADP reactivated channel activity, it did not fully prevent run-down. For these reasons most experiments performed to test the effect of MgADP and sulphonylureas with R54 mutants were carried out using the R54 cysteine mutation.

These results are consistent with the hypothesis (Schulze *et al.* 2003) that R54 interacts directly with PIP_2, but they also indicate that R54 is not required for functional coupling between Kir6.2 and SUR1, and that MgADP-dependent modulation of channel activity by SUR1 is independent of the R54–PIP_2 interaction.

Figure 8 illustrates the effects of R54 mutations with SUR1 on single-channel kinetics. These experiments could only be performed with SUR1, because channel activity could not be recorded in the absence of SUR1. Unlike R176E + SUR1 or R176E/R177E + SUR1 channels, which prevented long bursts so that only brief openings were observed, long bursts still occurred in R54E + SUR1 channels. However, the duration of the bursts was shorter, and separated by longer closed times (Table 1). Closed times were fitted by two exponentials with time constants of 0.6 and 23 ms. The fast time constant, corresponding to closed times within bursts, was similar to that of wild-type channels. However, the slow time constant (not well-illustrated in Fig. 8, because it accounted for only a small percentage of the maximum count), which corresponded to closed times between bursts, was 2–3 times longer than in wild-type Kir6.2 + SUR1 channels.

Thus, the interaction of R54 with PIP_2 modulates the ability of SUR1 to induce long bursting behaviour in Kir6.2 + SUR1 channels, but to a lesser extend than the interaction of PIP_2 with R176 and/or R177.

Discussion

We carried out a number of experiments with Kir6.2 channel mutants to further understand how SUR1 and PIP_2 regulate channel activity, and how their actions may be interrelated. It had been previously shown that bursting behaviour in Kir6.2 is facilitated by mutations at C166, as C166A/S increases P_o to near maximal (0.8) by inducing constant bursting even in the absence of SUR1 (Trapp *et al.* 1998). Here we have shown that bursting requires the interaction of PIP_2 with the Kir6.2 residues R176/R177, as C166A/R176E/R177E channels exhibit only short openings even in the presence of SUR1, although they remained functionally coupled to SUR1, as shown by intact MgADP and sulphonylurea sensitivity. Based on these observations, we conclude that mutations at C166 must act together with the R176/R177–PIP_2 interaction to generate bursts of openings. Although it also modulates bursting kinetics, the other PIP_2-binding residue, R54, has less of an effect on burst duration. R206 may be also critical for PIP_2 regulation (Shyng *et al.* 2000; John *et al.* 2001), but we could not assess its role because mutations at this position did not yield functional channels even though they are inserted into the plasma membrane (data not shown).

Like C166 mutations, one major effect of SUR1 is to induce bursting. However, SUR1 only increases P_o from 0.1–0.2 to 0.3–0.5, much less than the maximal P_o of C166A channels. In the presence of MgADP or MgUDP, however, P_o approaches a maximum value (Alekseev *et al.* 1998) similar to C166A. It follows that SUR1 must increase the P_o of Kir6.2 via two mechanisms. The first is a direct mechanism, similar, but less potent than in C166A, which may involve interaction between transmembrane domains of Kir6.2 and SUR1 (Babenko & Bryan, 2003), requires an intact PIP_2 interaction with R176/177, and is MgADP-independent. The second is an indirect mechanism, which is MgADP-dependent and may involve the distal N-terminus of Kir6.2, as deleting the latter region eliminates both MgADP and

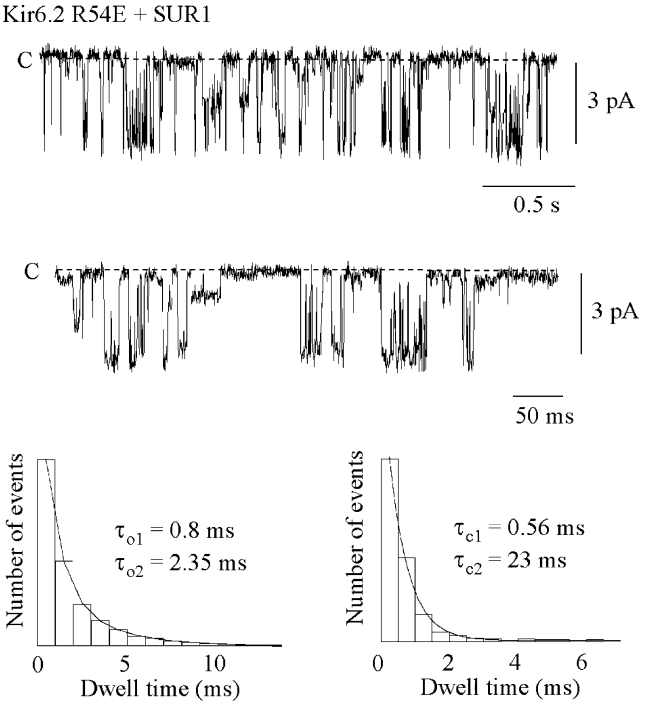

Figure 8. Single-channel recordings from R54E + SUR1 channels
Inward currents were recorded in excised inside-out patches at a holding potential of −60 mV and are represented as downward deflections. The lower record shows data on an expanded timescale. The open-time histogram on the left was fitted with a single exponential (τ_o = 2.3 ms). The closed-time histogram required two exponentials (τ_{c1} = 0.6 ms and τ_{c2} = 23 ms). The relative contribution of these two components is given in Table 1.

sulphonylurea sensitivity (Babenko *et al.* 1999; Reimann *et al.* 1999; Koster *et al.* 1999*a*). The role of the interaction of R176 and R177 with PIP_2 in Kir6.2 channel regulation has been acknowledged previously (Fan & Makielski, 1997) and a negative charge at these position blocks Kir6.2 + SUR1 channel activity. However, our data presented here demonstrate that R176E and/or R177E did not affect MgADP-dependent activation of K_{ATP} channels. Therefore, it follows that the direct effect of SUR1 on K_{ATP} channel bursting requires the interaction of R176/R177 with PIP_2, while MgADP-dependent regulation is independent of this interaction. As shown in Fig. 9, these two processes may act together to confer maximal channel P_o to wild-type Kir6.2 channels. Thus, when PIP_2 affinity is low, as in R54X or R176X/R177X mutants, the MgADP-dependent activation prevails and channel inhibition by sulphonylureas is very potent. In contrast, when the apparent affinity of PIP_2 is high, as with C166A, the stimulatory effect of the MgADP-dependent process is minimal and sulphonylureas have little apparent inhibitory effect.

A model of K_{ATP} channel regulation by adenine nucleotides, SUR1 and PIP_2

We previously proposed a minimal kinetic model to account for regulation of the K_{ATP} channel by ATP (John *et al.* 2003). Based on our analysis of the effects of adenine nucleotides, we proposed that K_{ATP} channels transition between a stable open state (O_s), an unstable open state (O_u), an unstable closed state (C_u) and a stable closed state (C_s), and that the phosphate groups of ATP interact with positively charged residues in Kir6.2 to shift the equilibrium towards the closed states, as shown in Fig. 9. For simplification, we previously omitted the fifth state (C_f), which mediates the brief ATP-independent closings during bursts when the channel is in the O_S state.

This model can be readily adapted to explain how PIP_2, SUR1, MgADP and sulphonylureas regulate the channel. When the channel is interacting with PIP_2 at the R176/R177 sites, either SUR1 or C166 mutations facilitate the O_u to O_s transition, promoting entry into the bursting states (O_s and C_f). However C166 mutations are more effective than SUR1 at inducing bursting, in part because SUR1 interacts with the N-terminus of Kir6.2 (Babenko *et al.* 1999; Reimann *et al.* 1999; Koster *et al.* 1999*a*) to inhibit the C_u to O_u transition. MgADP binding to SUR1 relieves this inhibition, maximizing P_o by pushing the channel towards the open states. Sulphonylureas, on the other hand, reverse the effect of MgADP and facilitate the inhibitory interaction of the N-terminus to favour further the C_u state.

Figure 10 shows simulated single-channel activity generated with this model. Alteration of only two rate constants was sufficient to reproduce all of the effects of SUR1, PIP_2, MgADP, sulphonylureas and the C166A and R176/R177/R54 mutations on channel P_o and kinetics (see Appendix for further details). More precisely, simulations

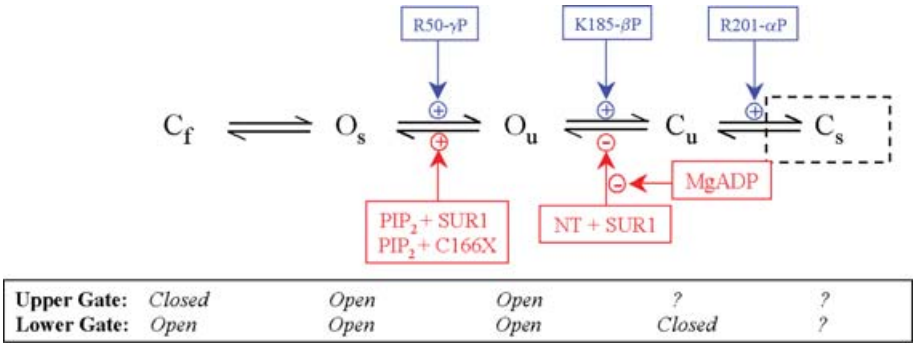

Figure 9. Schematic diagram of channel regulation by ATP, SUR, MgADP and PIP_2 based on a five-state model

The model is based on a previously proposed minimal model to account for adenine nucleotide sensitivity of Kir6.2 + SUR1 (John *et al.* 2003), with putative interactions of the α, β and γ phosphate groups of ATP with Kir6.2 residues indicated in blue. The ATP-bound states and the C_s state used previously are not included in the present modelling because the experiments were carried out in the absence of ATP; in the absence of ATP the C_s state is almost never visited. We incorporate into this model the regulatory effect of SUR1, PIP_2, MgADP and sulphonylureas as follows. In the absence of SUR1 or C166A, the channel transitions with fast kinetics between the O_u and C_u states, in which the lower gate (near the bundle-crossing or G-loops) is unstable. In the presence of SUR1 or when C166 is mutated to C166A/S, channel interaction with PIP_2 stabilizes the lower gate, so that the channel enters the bursting states O_s and C_f, in which opening and closing transitions are mediated by the upper gate (at the selectivity filter). A second effect of SUR1, which involves the inhibitory effect of the N-terminus on channel gating, takes place at the C_u to O_u transition, such is relieved when MgADP binds to SUR1, thus, causing maximal channel activation. The effect of MgADP is inhibited by sulphonylureas, decreasing channel P_o. Simulations related to this model are shown in Fig. 10.

of the stimulatory effects of SUR1 and C166A, which reflect channel interaction with PIP_2, required increasing the transition rate between O_u and O_s (Fig. 10*B* and *E* compared to *A*), while stimulation by MgADP and inhibition by sulphonylureas required increasing and decreasing the transition rate from C_u to O_u, respectively (Fig. 10*B* and *D* compared to *C*). The latter results are very similar to previously published data (Alekseev *et al.* 1998). Thus, the model in Fig. 9, which was originally formulated as a minimal model to account for the effects of adenine nucleotides on channel activity (John *et al.* 2003), also accommodates the major findings of the present study.

This kinetic model is also consistent with speculations about the physical nature of gates in Kir channels. It has been hypothesized that Kir channels have an upper gate at the selectivity filter and a lower gate below the selectivity filter. The lower gate may be located near the bundle crossing, where the M2 transmembrane segments cross near the membrane–cytoplasm interface (Phillips & Nichols, 2003; Proks *et al.* 2003; Xiao *et al.* 2003), or, alternatively, may involve the recently described G-loops (Pegan *et al.* 2005). In our model, C_f and O_s correspond to the closed and open positions of the upper gate at the selectivity filter when the lower gate is open, whereas O_u and C_u correspond to the open and closed states of the lower gate, respectively (Fig. 9). One possibility is that SUR1 or C166A/S mutations stabilize the lower gate in an open configuration (the O_s state) by strengthening the interaction of PIP_2 with R176 and R177, which are located near the bundle crossing. If the lower gate near the bundle crossing is not stabilized, for instance when R176/R177 are mutated or when SUR1 is not present, bursts are inhibited. Supporting this possibility, open and closed kinetics from outside the bursts (τ_o, 0.7 ms; τ_c, 15 ms), which are different from intraburst kinetics (τo, 2.2 ms; τc, 0.6 ms), are observed with Kir6.2 alone and R176E/R177E mutants coexpressed with SUR1. Based on these observations, we hypothesize that in the absence of strong channel interaction with PIP_2, instability of the lower gate limits ion permeation either directly, or indirectly by inducing closure of the upper gate at the selectivity filter.

Summary

The data presented here are consistent with a model in which entry into the high P_o bursting state is controlled by SUR1 or C166 mutations in a manner dependent on the interaction of PIP_2 with R176, R177 and, to a lesser extent, R54. We speculate that the interaction with PIP_2 stabilizes the bundle crossing in an open state, corresponding to channel bursting. SUR1 also increases channel activity via a second process regulated by MgADP, but not PIP_2. Sulphonylureas decrease P_o by inhibiting this process.

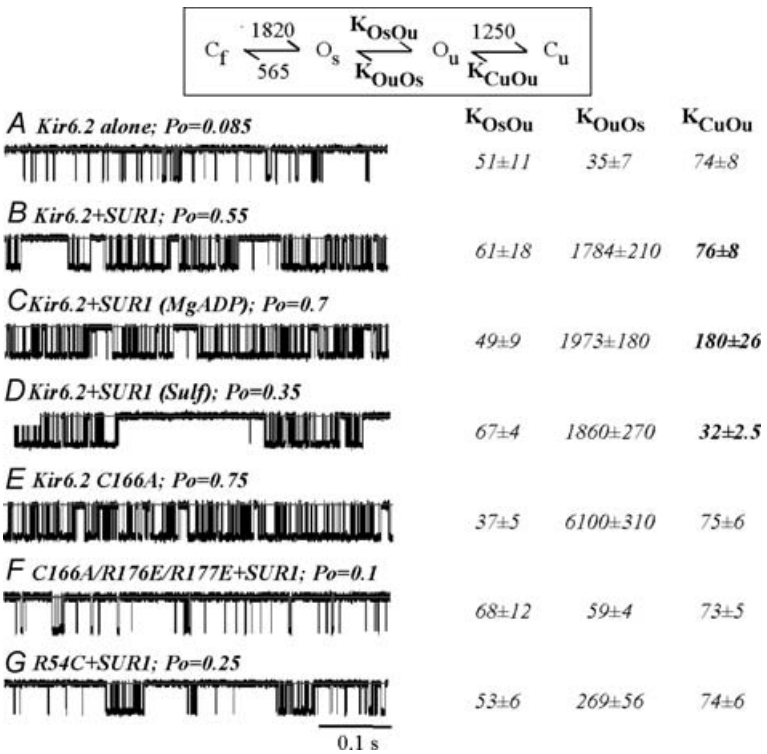

Figure 10. Simulation of single channel kinetic behaviour using the model in Fig. 9
The numbers in the reaction scheme at the top indicate rate constants (in units of s^{-1}) that were fixed throughout the simulations. The values for the O_s to C_f and C_f to O_s transitions were obtained using C166A mutant data and are similar to those published by other investigators (see Appendix). The values for the other rate constants (K_{OsOu}, K_{OuOs} and K_{CuOu}), which were fitted to simulate different conditions in *A*–*G*, are shown in italics at the right of each simulated single-channel current tracing. Fitting to the model shown at the top was carried out using the MIL function of the QuB software (University at Buffalo, NY, USA). Interventions in *A* and *E*–*G* could be fitted by changes of one rate constant, K_{OuOs}, reflecting the channel's affinity for PIP_2. In *B*–*D*, illustrating the effects of SUR1 (*B*), SUR1 + MgADP (*C*) and SUR1 + sulphonylurea (*D*), all the data could be fitted by changes of the K_{CuOu} value (bold characters). Channel P_o values were calculated for each experimental condition and are indicated above each single channel current trace. See Discussion and Appendix for further details.

Appendix

A five-state model incorporating the regulation by SUR1 and PIP_2

Previous models accounting for burst of openings have used the following four states:

$$C_f \rightleftharpoons O \rightleftharpoons C_1 \rightleftharpoons C_2$$

The C_f state accounts for the fast opening and closing during the burst, the O state accounts for the open state, the C_1 state accounts for the closure outside the bursts and the C_2 state is the ATP-dependent closed state. However, analysis of single K_{ATP} channel behaviour in β cells (Ribalet *et al.* 1989) or cloned Kir6.2 + SUR1 channels (Drain *et al.* 1998; John *et al.* 1998) revealed that the kinetics of fast events occurring outside the burst are different from those within the burst. Thus, while the open and closed times outside the burst are best fitted with the time constants $\tau_o = 0.6$ ms and $\tau_c = 15$ ms, the open and closed time constants within the burst are 2 ms and 0.6 ms, respectively. Based on these observations we propose the model with two open states that is presented in Fig. 9, where the fast transition between C_u (closed unstable state) and O_u (open unstable state) reflects motion of the lower gate near the bundle crossing, which upon stabilization by PIP_2 allows for the transition to the O_s (open stable state) and the bursting kinetics ($C_f \leftrightarrow O_s$).

Following these assumptions, the rate constants shown in Fig. 10 were obtained as follows. First, the single-channel data obtained from C166A, which bursts almost continuously, were fitted to obtain the $C_f \leftrightarrow O_s$ rate constants. These rate constants are very similar to those reported by other investigators (Alekseev *et al.* 1998; Trapp *et al.* 1998; Fan & Makielski, 1999; Enkvetchakul *et al.* 2000; Lin *et al.* 2003). The backward rate constant O_u to C_u was estimated as 1250 s^{-1} to account for the short channel open time (0.6–0.7 ms) in the absence of SUR1 or the decreased apparent affinity of PIP_2 (R176E/R177E).

With these three rate constants, fixed model optimization was carried out using the QuB suite of programs to estimate the three other transition rates under the various experimental conditions outlined in Fig. 10. Once these rates were determined, simulations were carried out and the outcome compared to the experimental data (left panel in Fig. 10).

The most prominent results of our simulations are as follows. Decrease of the forward rate constant K_{OuOs} from approximately 6000 s^{-1} with C166A (10E) to 50 s^{-1} with R176E/R177E (Fig. 10*F*) underlies the transition from constant bursting to fast channel gating. Thus, when continuous bursting was generated, with C166A channels, the mean open time approached 2 ms. In contrast, with decreased PIP_2 interaction (Fig. 10*F*) or absence of SUR1 (Fig. 10*A*), rapid channel gating yielded a mean open time approaching the experimental value of 0.6 ms, consistent with two kinetically distinct open states. The simulation also yielded fast openings between bursts with R54C + SUR1 (Fig. 10*G*) that could not be simulated in the absence of the unstable open state (O_u). Thus, K_{OuOs}, or more precisely the ratio K_{OsOu}/K_{OuOs} which reflects the affinity of the channel for PIP_2, controls the transition from fast channel kinetics to bursting. A low value for this ratio, corresponding to stabilization of the lower gate, results in bursting, while a high value concurrent with gate destabilization results in fast channel kinetics. Greatest stabilization is obtained with C166A (Fig. 10*E*), SUR1 yields an intermediary value (Fig. 10*B*) and R176E/R177E or Kir6.2 in the absence of SUR1 yields similar, low values.

While most interventions (Fig. 10*A*, *B* and *E*–*G*) could be simulated by varying K_{OuOs} or the K_{OsOu}/K_{OuOs} ratio, the effects of MgADP and sulphonylureas, which affect the 'long' closed time between bursts of opening, were best simulated by changes in K_{CuOu}. In Fig. 10, these changes are shown in bold characters. Thus, increase of K_{CuOu} from 76 s^{-1} (Fig. 10*B*) to 180 s^{-1} (Fig. 10*C*), which corresponds to addition of MgADP-dependent stimulation, yielded almost continuous bursting even though K_{OuOs} remained at a relatively low level. In contrast, the effect of the sulphonylureas, which block channel stimulation by MgADP, was fitted with a decrease in K_{CuOu} from 76 s^{-1} (Fig. 10*B*) to 32 s^{-1} (Fig. 10*D*). These values for the effects of MgADP and sulphonylureas are very similar to previously published data (Alekseev *et al.* 1998; transition from O to C_2 state).

The results of these simulations support our hypothesis whereby a transition between fast channel gating and bursting is controlled by stabilization of the lower gate (increase in K_{OuOs}) in a PIP_2-dependent manner. In conjunction with this process, MgADP favours bursting by relieving the inhibitory effect of the N-terminus and thus increases K_{CuOu}; sulphonylureas reverse this process.

References

Alekseev AE, Brady PA & Terzic A (1998). Ligand-insensitive state of cardiac ATP-sensitive K^+ channels. Basis for channel opening. *J Gen Physiol* **111**, 381–394.

Babenko AP & Bryan J (2003). Sur domains that associate with and gate K_{ATP} pores define a novel gatekeeper. *J Biol Chem* **278**, 41577–41580.

Babenko AP, Gonzalez G & Bryan J (1999). The N-terminus of KIR6.2 limits spontaneous bursting and modulates the ATP-inhibition of KATP channels. *Biochem Biophys Res Commun* **255**, 231–238.

Baukrowitz T, Schulte U, Oliver D, Herlitze S, Krauter T, Tucker SJ, Ruppersberg JP & Fakler B (1998). PIP2 and PIP as determinants for ATP inhibition of KATP channels. *Science* **282**, 1141–1144.

Drain P, Li L & Wang J (1998). KATP channel inhibition by ATP requires distinct functional domains of the cytoplasmic C terminus of the pore-forming subunit. *Proc Natl Acad Sci U S A* **95**, 13953–13958.

Enkvetchakul D, Loussouarn G, Makhina E, Shyng SL & Nichols CG (2000). The kinetic and physical basis of K(ATP) channel gating: toward a unified molecular understanding. *Biophys J* **78**, 2334–2348.

Fan Z & Makielski JC (1997). Anionic phospholipids activate ATP-sensitive potassium channels. *J Biol Chem* **272**, 5388–5395.

Fan Z & Makielski JC (1999). Phosphoinositides decrease ATP sensitivity of the cardiac ATP-sensitive K^+ channel. A molecular probe for the mechanism of ATP-sensitive inhibition. *J Gen Physiol* **114**, 251–269.

Graham FL & van der Eb AJ (1973). Transformation of rat cells by DNA of human adenovirus 5. *Virology* **54**, 536–539.

John SA, Monck JR, Weiss JN & Ribalet B (1998). The sulphonylurea receptor SUR1 regulates ATP-sensitive mouse Kir6.2 K^+ channels linked to the green fluorescent protein in human embryonic kidney cells (HEK 293). *J Physiol* **510**, 333–345.

John SA, Weiss JN & Ribalet B (2001). Regulation of cloned ATP-sensitive K channels by adenine nucleotides and sulfonylureas: interactions between SUR1 and positively charged domains on Kir6.2. *J Gen Physiol* **118**, 391–405.

John SA, Weiss JN, Xie LH & Ribalet B (2003). Molecular mechanism for ATP-dependent closure of the K^+ channel Kir6.2. *J Physiol* **552**, 23–34.

Koster JC, Sha Q & Nichols CG (1999*a*). ATP inhibition of KATP channels: control of nucleotide sensitivity by the N-terminal domain of the Kir6.2 subunit. *J Physiol* **515**, 19–30.

Koster JC, Sha Q, Shyng S & Nichols CG (1999*b*). Sulfonylurea and K^+-channel opener sensitivity of K_{ATP} channels: functional coupling of Kir6.2 and SUR1 subunits. *J Gen Physiol* **114**, 203–213.

Kuo A, Gulbis JM, Antcliff JF, Rahman T, Lowe ED, Zimmer J, Cuthbertson J, Ashcroft FM, Ezaki T & Doyle DA (2003). Crystal structure of the potassium channel KirBac1.1 in the closed state. *Science* **300**, 1922–1926.

Lin YW, Jia T, Weinsoft AM & Shyng SL (2003). Stabilization of the activity of ATP-sensitive potassium channels by ion pairs formed between adjacent Kir6.2 subunits. *J Gen Physiol* **122**, 225–237.

MacGregor GG, Dong K, Vanoye CG, Tang L, Giebisch G & Hebert SC (2002). Nucleotides and phospholipids compete for binding to the C terminus of KATP channels. *Proc Natl Acad Sci U S A* **99**, 2726–2731.

Nishida M & MacKinnon R (2002). Structural basis of inward rectification: cytoplasmic pore of the G protein-gated inward rectifier GIRK1 at 1.8 A resolution. *Cell* **111**, 957–965.

Pegan S, Arrabit C, Zhou W, Kwiatkowski W, Collins A, Slesinger PA & Choe S (2005). Cytoplasmic domain of Kir2.1 and Kir3.1 show sites for modulating gating and rectification. *Nat Neurosci* **8**, 279–287.

Phillips LR & Nichols CG (2003). Ligand-induced closure of inward rectifier Kir6.2 channels traps spermine in the pore. *J Gen Physiol* **122**, 795–804.

Proks P, Antcliff JF & Ashcroft FM (2003). The ligand-sensitive gate of a potassium channel lies close to the selectivity filter. *EMBO Rep* **4**, 70–75.

Reimann F, Tucker SJ, Proks P & Ashcroft FM (1999). Involvement of the n-terminus of Kir6.2 in coupling to the sulphonylurea receptor. *J Physiol* **518**, 325–336.

Ribalet B, Ciani S & Eddlestone GT (1989). ATP mediates both activation and inhibition of K(ATP) channel activity via cAMP-dependent protein kinase in insulin-secreting cell lines. *J Gen Physiol* **94**, 693–717.

Ribalet B, John SA & Weiss JN (2000). Regulation of cloned ATP-sensitive K channels by phosphorylation, MgADP, and phosphatidylinositol bisphosphate (PIP(2)): a study of channel rundown and reactivation. *J Gen Physiol* **116**, 391–410.

Ribalet B, John SA & Weiss JN (2003). Molecular basis for Kir6.2 channel inhibition by adenine nucleotides. *Biophys J* **84**, 266–276.

Schulze D, Krauter T, Fritzenschaft H, Soom M & Baukrowitz T (2003). Phosphatidylinositol 4,5-bisphosphate (PIP2) modulation of ATP and pH sensitivity in Kir channels. A tale of an active and a silent PIP2 site in the N terminus. *J Biol Chem* **278**, 10500–10505.

Shyng SL, Cukras CA, Harwood J & Nichols CG (2000). Structural determinants of PIP(2) regulation of inward rectifier K(ATP) channels. *J Gen Physiol* **116**, 599–608.

Trapp S, Proks P, Tucker SJ & Ashcroft FM (1998). Molecular analysis of ATP-sensitive K channel gating and implications for channel inhibition by ATP. *J Gen Physiol* **112**, 333–349.

Tucker SJ, Gribble FM, Zhao C, Trapp S & Ashcroft FM (1997). Truncation of Kir6.2 produces ATP-sensitive K^+ channels in the absence of the sulfonylurea receptor. *Nature* **387**, 179–183.

Xiao J, Zhen XG & Yang J (2003). Localization of PIP2 activation gate in inward rectifier K^+ channels. *Nat Neurosci* **6**, 811–818.

Acknowledgements

This work was supported by National Institutes of Health (NIH) grants R37HL60025 and NIH SCOR (Specialized Center of Research) in Sudden Cardiac Death P50 HL52319, and Laubisch and Kawata Endowments to J.N.W, and by a Grant-in-Aid from the American Heart Association (Western States Affiliate) to L-H.X.